



Hill, C., Czajka, A., Hazell, G., Grillo, I., Rogers, S. E., Skoda, M. W. A., ... Eastoe, J. (2018). Surface and bulk properties of surfactants used in fire-fighting. *Journal of Colloid and Interface Science*, 530, 686-694.
<https://doi.org/10.1016/j.jcis.2018.07.023>

Peer reviewed version

License (if available):
CC BY-NC-ND

Link to published version (if available):
[10.1016/j.jcis.2018.07.023](https://doi.org/10.1016/j.jcis.2018.07.023)

[Link to publication record in Explore Bristol Research](#)
PDF-document

This is the author accepted manuscript (AAM). The final published version (version of record) is available online via Elsevier at <https://www.sciencedirect.com/science/article/pii/S0021979718307793?via%3Dihub>. Please refer to any applicable terms of use of the publisher.

University of Bristol - Explore Bristol Research

General rights

This document is made available in accordance with publisher policies. Please cite only the published version using the reference above. Full terms of use are available:
<http://www.bristol.ac.uk/pure/about/ebr-terms>

Surface and Bulk Properties of Surfactants used in Fire-Fighting

Christopher Hill^a, Adam Czajka^a, Gavin Hazell^a, Isabelle Grillo^b, Sarah E. Rogers^c, Maximilian W. A. Skoda^c, Nigel Joslin^d, John Payne^d, Julian Eastoe^{a,*}

^a*School of Chemistry, University of Bristol, Cantock's Close, Bristol, BS8 1TS, UK*

^b*Institut Laue-Langevin, 71 avenue des Martyrs - CS 20156, 38042 Grenoble Cedex 9, France*

^c*ISIS Pulsed Neutron and Muon Source, Science and Technology Facilities Council, Rutherford Appleton Laboratory, Harwell, UK*

^d*Angus Fire Ltd., Station Road, Bentham, LA2 7NA, UK*

Abstract

Hypothesis: Reports on the colloidal and interfacial properties of fluorocarbon (FC) surfactants used in fire-fighting foam formulations are rare. This is primarily because these formulations are complex mixtures of different hydrocarbon (HC) and fluorocarbon (FC) surfactants. By developing a greater understanding of the individual properties of these commercial FC surfactants, links can be made between structure and respective surface/ bulk behaviour. Improved understanding of structure property relationships of FC surfactants will therefore facilitate the design of more environmentally responsible surfactant replacements.

Experiments: Surface properties of three partially fluorinated technical grade surfactants were determined using tensiometry and neutron reflection (NR), and compared with a research-grade reference surfactant (sodium perfluorooctanoate (NaPFO)). To investigate the bulk behaviour and self-assembly in solution, small-angle neutron (SANS) scattering was used.

Findings: All FC surfactants in this study generate very low surface tensions ($< 20 \text{ mN m}^{-1}$) which are comparable, and in some cases, lower than fully-fluorinated surfactant analogues. The complementary techniques (ten-

*Corresponding Author

Email address: julian.eastoe@bristol.ac.uk (Julian Eastoe)

siometry and NR) allowed direct comparison to be made with NaPFO in terms of adsorption parameters such as surface excess and area per molecule. Surface tension data for these technical grade FC surfactants were not amenable to reliable interpretation using the Gibbs adsorption equation, however NR provided reliable results. SANS has highlighted how changes in surfactant head group structure can affect bulk properties. This work therefore provides fresh insight into the structure property relationships of some industrially relevant FC surfactants, highlighting the properties which are essential for development of more environmentally friendly replacements.

Keywords: Fluorocarbon Surfactants, Self-assembly, Neutron reflection, Small-angle neutron scattering, Fire-fighting foam formulations

1. Introduction

Hydrocarbon fuel fires pose a serious threat and as such require a rapid response. Hence, effective and efficient fire-extinguishing agents are needed to prevent re-ignition of fires. Historically, water has long been used for suppressing fires, however it is ineffective for oily liquid fuel fires [1]. Early advances (1920s - 1950s) in fire-fighting found that incorporation of proteinacious materials, such as hydrolysed hoof and horn meal, as well as other natural products, namely saponine or liquorice were beneficial [1, 2]. The 1960s saw progress mainly in the use of synthetic surfactant formulations, which lead to the development of what are now known as aqueous film forming foams (AFFFs). AFFFs were and still are the most effective formulations for extinguishing fires involving flammable liquid fuels [3]. As with most commercial formulations, AFFFs comprise complex mixtures, incorporating major components such as a solvent (typically a glycol ether), fluorocarbon (FC) (perfluorinated anionic and partially fluorinated amphoteric) surfactants, and hydrocarbon-based surfactants. Table S1 in supporting information shows the composition of a typical AFFF formulation in terms of percentage composition.

Fluorocarbon (FC) surfactants are distinctly different from hydrocarbon (HC) surfactants in various respects. Although the polar headgroups of HC and FC surfactants may be similar, non-polar FC tails have both hydrophobic and oleophobic (oil-repelling) properties, compared to HC surfactants which are considered only hydrophobic [4]. Hence, FC surfactants exhibit both hydrophobic and oleophobic characteristics, which in fire-fighting applications, account for their effectiveness. In addition to this, FC surfactants generally

display greater surface activity compared to HC analogues. Fluorine has a lower polarisability than hydrogen; therefore, the total dispersion interaction is lower for the interaction between fluorinated chains. Hence, FC surfactants are expected to have weaker attractive intermolecular forces than similar HC surfactants. In comparison to those of analogous HC, FC surfactants have larger volume of perfluoroalkyl moieties and larger limiting cross-sectional area [4, 5]. As a result, FC surfactants show an enhanced tendency to self-assemble, and collect at the air-water interface to reduce the surface energy. For this reason, incorporation of FC surfactants into AFFFs leads to an increase in spreading coefficient over a hydrocarbon fuel surface, therefore leading to more efficient extinguishment. More information can be found in the following references [6, 7, 8].

Although FC surfactants have many useful interfacial properties, and appear in a diverse range of applications, it has been known for many years that they are not environmentally friendly [9, 10, 11]. For example, It has been identified that FC with C_8 - C_{15} chain lengths are hazardous pollutants [12]. These molecules eventually break down to form PFOS (perfluorooctanesulphonate) and PFOA (perfluorooctanoic acid), which are recognised as having negative impacts on the environment and human health due to pronounced persistence, variable degrees of bioaccumulation potential and toxicity [3, 12]. Although new FC surfactants have been designed which are not bioaccumulative or toxic [13], the strength of the C-F bond hinders biodegradability.

The current understanding underpinning the use of AFFFs for fire-fighting applications is primitive and largely empirically based. As a result of this, few attempts have been made to model or investigate the behaviour of fire-fighting foam formulations from chemical perspectives [14, 15, 16]. Therefore, it is important to develop a more fundamental understanding of how the surfactants adsorb and self-assemble, both individually and as mixed systems in mimics of the real formulations (F/F mixtures and F/H mixtures).

This study is based on understanding the important structure-property relationship of individual FC surfactants used in typical fire-fighting foam applications. Studies with techniques such as force tensiometry, neutron reflection and small-angle neutron scattering have allowed the determination of the important properties typical AFFF FC surfactants possess from a chemical perspective. As well, this work demonstrates how changing the head group on a FC surfactant (anionic, non-ionic and zwitterionic) feeds through to marked changes to the interfacial properties of the surfactants.

2. Materials and Methods

2.1. Materials

All fluorinated surfactants, apart from sodium perfluorooctanoate (NaPFO), used in this study were provided by Angus Fire Ltd. DynaxTM DX1030 is a C6 anionic fluorosurfactant (IUPAC Name: 2-methyl-2-(3-((1H,1H,2H,2H-perfluoro-1-octyl)thio)propanamido)propane-1-sulfonate), DynaxTM DX2200 is a C8 non-ionic fluorosurfactant and CapstoneTM 1157 is a C6 zwitterionic fluorosurfactant (IUPAC Name: N-(carboxymethyl)-N,N-dimethyl-3-(1H,1H,2H,2H-perfluoro-1-octanesulfonamido)propan-1-aminium) DynaxTM is a trademark of Dynax Corporation and CapstoneTM is a trademark of The Chemours Company. Surfactants were provided as liquid formulations, acetone was added as a non-solvent to induce precipitation of the solid surfactants for purification. Characterisation and chemical analysis were used to assess purity of the precipitated FC surfactants (supporting information). NaPFO (CAS 335-95-5) was prepared and purified by the following method. Perfluorooctanoic acid (CAS 335-67-1) of stated purity $\geq 99\%$ was obtained from Fluorochem, converted into the appropriate metal salt by reaction with the stoichiometric amount of hydroxide, and purified by recrystallisation from a mixture of ethanol and propanol (1:1, vol:vol). Further purification included Soxhlet extraction, with ethyl acetate, to remove residual inorganic material, and foam fractionation to remove hydrophobic impurities (following method in ref [17]). Pyrene (Acros, puriss $\geq 99\%$), deuterium oxide (Aldrich, 99.9%) were used as received.

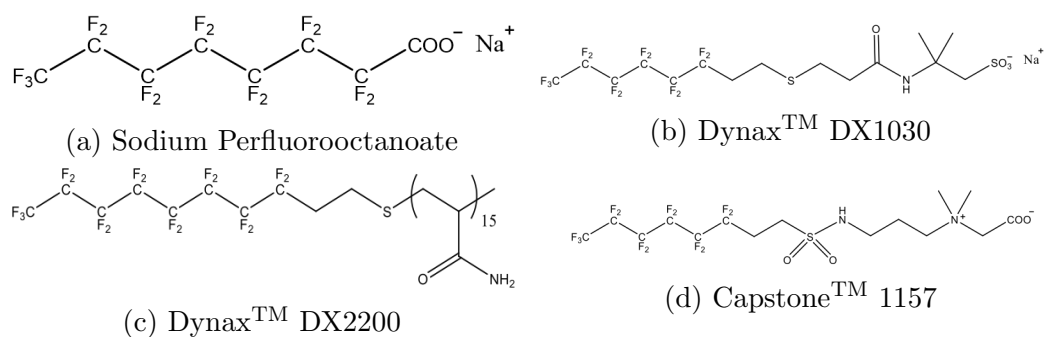


Figure 1: Surfactants Used In This Work

2.2. Methods

2.2.1. Surface Tension Measurements

Surface tension measurements were carried out on a Krüss K100 force tensiometer using the Wilhemy plate method at 25 °C. Glassware was washed thoroughly with a dilute Decon solution and then with wash cycles of methanol and ultra pure water (Millipore, 18.2 MΩ cm). The cleaning cycles were repeated until the surface tension of water was returned as 72 ± 0.2 mN m⁻¹.

Stock surfactant solutions were prepared and aliquots were added to deionised water to give desired concentrations. Each concentration measurement was repeated over a period of up to 30 minutes to ensure equilibration. Attempts were made to model the data using the Gibbs adsorption isotherm, which relates the surface excess, inversely proportional to the area per molecule, to changes in the surface tension with concentration:

$$\Gamma = -\frac{1}{mRT} \frac{d\gamma}{d\ln C} \quad (1)$$

$$A_{cmc} = \frac{1}{\Gamma_{cmc} N_A} \quad (2)$$

where Γ is the surface excess, Γ_{cmc} is the surface excess at the critical micelle concentration (CMC), A_{cmc} is the area per molecule at the CMC, R is the gas constant, T is temperature, γ is surface tension, C is concentration and N_a is the Avogadro's number. The prefactor m is dependent on the surfactant type and structure, as well as the presence of extra electrolyte in the aqueous phase [18]. For non-ionic and zwitterionic surfactants, a value of 1 for the pre-factor has been confirmed [19, 20], as well for 1:1 ionic surfactants, in the absence of extra electrolyte, has also been confirmed [18]. Recently, it has been shown that traces of multivalent ionic impurities can lead to changes in the prefactor, therefore leading to problems employing the Gibbs adsorption isotherm [21]. In this study, a prefactor of 1 has been used for the non-ionic and zwitterionic surfactants, and a prefactor of 2 has been used for the anionic surfactants, following literature [18, 19, 20].

2.2.2. Fluorescence

Fluorescence measurements were carried out as described in ref [22]. Fluorescence measurements were carried out in quartz cuvettes at 25 °C on a Cary Eclipse (Varian) Fluorescence spectrometer. Pyrene was used as a fluorescent probe for determining CMCs of the studied surfactants. A fixed

concentration of pyrene (1.0×10^{-6} M) was added to sample vials from a known stock prepared in acetone. The acetone was allowed to evaporate off in air, leaving behind a known mass of the involatile pyrene, before the aqueous surfactant solution was added over the concentration range of interest. Fluorescence emission spectra were collected after excitation at $\lambda = 337$ nm, with a slit width of 5 nm for excitation and emission. Each measurement was repeated three times to ensure a stable value.

2.2.3. Neutron Reflection

Neutron reflection (NR) measurements were conducted using the INTER beam-line on Target Station 2 at the ISIS facility (Rutherford Appleton Laboratory, Didcot, UK) [23]. Measurements were taken using a single point detector and fixed grazing incidence angles (0.8° and 2.3°). The absolute reflectivity was calibrated with respect to the direct beam and the reflectivity from a clean D₂O surface. The NR experiments were carried out in two contrasts, D₂O and air contrast matched water (ACMW; 8 mol% D₂O in H₂O with an SLD of 0). A pipette was used on each sample to suck off any air bubbles and also to remove the initial surface layer in case any hydrophobic impurities were present. The data were fit using MOTOFIT, written for IGOR Pro [24].

Only the relevant theory is described here, but for a more in-depth account, the reader is referred to the following references [25, 26]. The specular reflection of neutrons is measured as a function of the scattering vector, Q , as given by:

$$Q = \frac{4\pi \sin\theta}{\lambda} \quad (3)$$

where λ is neutron wavelength, and θ is the angle of half the reflection. The experimental reflectivity is related to the square of the Fourier transform of the scattering length density (SLD), $\rho(z)$, normal to the surface. For neutrons, $\rho(z) = \sum_i n_i(z) \cdot b_i$, where n_i and b_i are the number density and scattering length of the i th component and z is the direction perpendicular to the surface [26]. For surfactant solutions the measured reflectivity curve can be modeled in terms of a single, uniform layer to fit for thickness, τ , and a scattering length density, ρ [25]. These values are related to the surface coverage, Γ , and area per molecule, A , in the following way:

$$A = \frac{\sum b_i}{\rho\tau} = \frac{1}{\Gamma N_a} \quad (4)$$

where Σb_i is the sum of neutron scattering lengths of nuclei over the surfactant molecule, Γ is the surface coverage and N_a is Avogadro's number.

2.2.4. Small-Angle Neutron Scattering

SANS measurements were performed on SANS 2D at the ISIS facility (Rutherford Appleton Laboratory, Didcot, UK) and D33 at the Institut Laue-Langevin (ILL, Grenoble, France). On SANS 2D, a simultaneous Q -range of $0.004 - 0.6 \text{ \AA}^{-1}$ was achieved with a neutron wavelength range of $1.75 < \lambda < 15.5 \text{ \AA}$ and a source-sample-detector distance $L1 = L2 = 4 \text{ m}$. The D33 instrument used neutrons with a wavelength of $\lambda = 6 \text{ \AA}$ and two sample-detector positions (2 and 7.5 m) providing an accessible Q range of $0.005 - 0.2 \text{ \AA}^{-1}$. All samples were made in D_2O , using 2 mm path length rectangular quartz cells at a temperature of $25 \text{ }^\circ\text{C}$. Raw SANS data were reduced by subtracting the scattering of the empty cell and the D_2O background and normalised to an appropriate standard using the instrument-specific software. SANS data were fit using the analysis package SasView.

In a SANS experiment, the intensity (I) of scattered neutrons is measured as a function of momentum transfer (Q), see equation 3. For monodispered homogeneous scatterers of volume V_p , number density N_p and coherent scattering length density ρ_p , dispersed in a solvent of scattering length density ρ_s , the normalised SANS intensity $I(Q)$ (cm^{-1}) is:

$$I(Q) = \phi V_P (\rho_p - \rho_s)^2 P(Q) S(Q) \quad (5)$$

Where $\phi = (N/V) V_p$. The first three terms in equation 5 are independent of Q and account for the absolute intensity of scattering. The last two terms in the equation are Q -dependent functions. $P(Q)$ is the particle form factor, which describes intra-particle information such as size and shape. $S(Q)$ is the structure factor, which describes the scattering due to inter-particle correlations.

3. Results and Discussion

3.1. Equilibrium Surface Tensions and Critical Micelle Concentrations (CMCs)

Important parameters to determine for surfactants are how effective they are at reducing the aqueous surface tension and their critical micelle concentrations (CMC). In fire-fighting applications, properties such as foamability, foam stability and spreading are linked to surface tension reductions. For

example, it is often believed that employing surfactants at their CMCs gives the best foam performance [27].

Characterisation of the pure research-grade surfactant, sodium perfluorooctanoate (NaPFO) was compared to literature results [28, 29]. The same studies were carried out using the three technical grade fluorocarbon surfactants and the results are shown below.

3.1.1. Properties of NaPFO

Equilibrium γ vs. \ln (concentration) plots NaPFO is shown in Figure 2. The curve shows a clear break point at the CMC, with no minima or shoulders, which would be indicative of hydrophobic impurities. The CMC was determined by taking the second derivative of the γ vs. \ln (concentration) plots, and then applying a Gaussian distribution function, where the minimum was taken to be the value of the CMC. This method is described in supporting information [30]. Quartic functions were then fit through the pre-CMC data, to generate local tangents, then the Gibbs adsorption isotherm was used to estimate the surface excess (Γ_{cmc}) and the area per molecule (A_{cmc}) at the CMC using Equation 1, data shown in Table 1.

Surfactant	$\gamma_{CMC}/$ (mN m ⁻¹)	CMC/ (mM)	$\Gamma_{cmc}/$ (10 ⁻⁶ mol m ⁻²)	$A_{cmc}/$ (Å ²)
NaPFO (This Study)	22.6 ± 0.1	27.0 ± 0.2	4.1 ± 0.2	40 ± 2
NaPFO (Literature)	24.6	30.0	4.0	42

Table 1: Results from surface tension measurements of NaPFO from this study compared to literature [28, 29]

Similar results for NaPFO have been reported [28, 29] for both Γ_{cmc} and A_{cmc} and are comparable to the results achieved in this study. The results show a clear match between the data in this study and previous literature. This shows that the standard tensiometric method used here is amenable for analysis of pure research-grade fluorocarbon surfactant.

3.1.2. Technical Grade Surfactants

Equilibrium γ vs. \ln (concentration) plots for the three fire-fighting surfactants are shown in Figure 2. DynaxTM DX2200 (non-ionic) and CapstoneTM

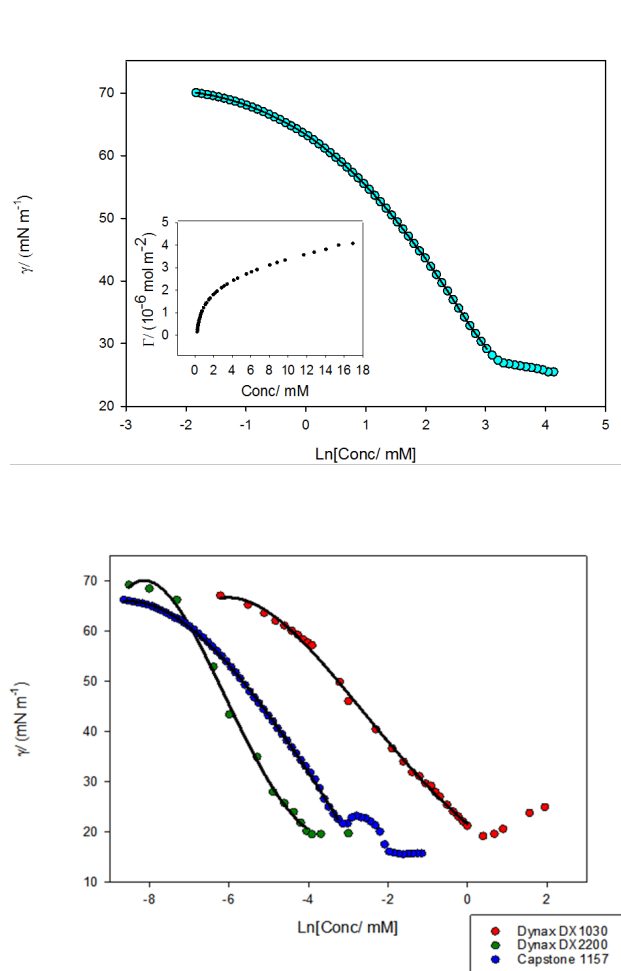


Figure 2: Above: Surface Tension vs. $\ln(\text{Concentration})$ for NaPFO, inset shows the adsorption isotherm of NaPFO. Below: Surface Tension vs. $\ln(\text{Concentration})$ Three Technical Grade Surfactants. $T = 25^\circ\text{C}$. Line fitted to pre-CMC data is a quartic function

1157 (zwitterionic) show clear break points at their respective CMCs, therefore relatively accurate CMC values can be determined. On the other hand, DynaxTM DX1030 (anionic) shows a minimum in the curve, followed by an increase in surface tension, which is indicative of hydrophobic impurities, as first recognised by Mysels *et al.* [31, 32]. CMCs were determined using the same method as previously mentioned, this is also true for calculation of both the surface excess (Γ_{cmc}) and the area per molecule (A_{cmc}), data shown

in Table S8 in the supporting information. Although it has been possible to attain CMC values, fluorescence probe measurements have been used to provide additional CMC values which were found to match well with the surface tension results (Table S9, supporting information).

Due to the nature of the surfactants, and the irregular forms of these surface tension isotherms (Figure S5), it is clear that problems will arise when attempting to use the Gibbs adsorption isotherm as described above. This is reflected in the erratic and sometimes unphysical data shown in Table S8 (supporting information), and obtained results should therefore be considered with caution. Taking the surface tension curve of DynaxTM DX1030 as an example, it can be seen that the line fitted through the data is straight, suggesting from the Gibbs adsorption isotherm that Γ is essentially constant. However is clearly not the case, as the surface tension is reducing. It might be expected that NaPFO and anionic DynaxTM DX1030 should achieve similar values for both surface excess and A_{cmc} due to their similar tail structures and head groups, however this is not the case. DynaxTM DX1030 was found to have an A_{cmc} two times larger and a surface excess \sim three times lower than SPFO, suggesting that use of the Gibbs adsorption isotherm for these technical grade surfactants should be treated with caution. In addition, anionic DynaxTM DX1030 and zwitterionic CapstoneTM 1157 are similar in both molecular size and level of fluorination (see Figure 1), therefore similar values for A_{cmc} and Γ_{cmc} would be expected. The anionic charge on DynaxTM DX1030 would be expected to cause an increase in A_{cmc} and thus decrease in Γ_{cmc} due to head group repulsion, however the difference observed between CapstoneTM 1157 and DynaxTM DX1030 does not fit in with this. DynaxTM DX2200 is non-ionic with repeating acrylamide units: a similar molecule was studied by Dupont *et al.* [33]. Their work was carried out with a tris(hydroxymethyl)acrylamidomethane (THAM)-derived telomer bearing a perfluorohexyl hydrophobic chain. In that case, $\Gamma_{cmc} = 2.68 \times 10^{-6}$ mol m⁻² and a A_{cmc} of 62 ± 2 Å², was observed.

Therefore, it seems that using tensiometric techniques and analysis with the Gibbs adsorption isotherm is not appropriate for accurate detail on the interfacial properties of these technical grade FC surfactants, resulting in unphysical values for both A_{cmc} and Γ_{cmc} . As a way to circumvent this issue and to determine these important information of interest, Neutron Reflection has been employed.

3.2. Neutron Reflection

Using NR with a fluorocarbon (FC) chain surfactants on air contrast match water (ACMW, i.e. $\rho_{ACMW} = 0 \text{ \AA}^{-2}$), the surface coverages can be determined directly from analyses of the reflectivity profiles $R(Q)$ [33, 34]. Data were modelled in terms of a single uniform layer to fit for monolayer thicknesses, τ , and scattering length densities ρ . Molecular areas and surface excesses were then calculated using the modelled parameters via Equation 4. The raw reflectivity curves can be found in the supporting information.

3.2.1. NaPFO

As for tensiometry, NaPFO was initially characterised to validate the method and ensure analyses. The parameters from analysis of the NaPFO $R(Q)$ data can be found in Table 2 and the Γ vs. concentration plot calculated using Equation 4 can be seen Figure S9 in the supporting information. Here, similar results have been reported when comparing to fitted parameters found in the literature [28, 29, 35].

Comparisons can also be made between NR and surface tension data in terms of both Γ_{cmc} and A_{cmc} . A high degree of agreement should be noted between these two complementary techniques: $\Gamma_{cmc} = 4.07 \pm 0.20 \times 10^{-6} \text{ mol m}^{-2}$ (ST) and $4.05 \pm 0.10 \times 10^{-6} \text{ mol m}^{-2}$ (NR), $A_{cmc} = 40 \pm 2 \text{ \AA}^2$ (ST) and $41 \pm 2 \text{ \AA}^2$ (NR). These results therefore show how using both standard tensiometric methods in conjunction with NR can provide directly comparable results and are therefore amenable for analysis of research-grade fluorocarbon surfactants.

3.2.2. Technical Grade Surfactants

It was previously shown that using common tensiometric techniques did not allow accurate analysis of parameters such as Γ_{cmc} and A_{cmc} for technical grade FC surfactants. Therefore, the basis of this section is to determine whether these important surfactant parameters can be obtained using NR. All surfactants studied in this section have been subject to the same analysis as previously in Section 3.2.1. Presented in Table 2 are the fitted values from analyses of the NR data. The full set of parameters used to fit this data can be found in the supporting information. Comparing the results for the technical grade surfactants with the NaPFO, it can be seen that as might be expected owing to the similarities in chemical structure (Figure 1) DynaxTM DX1030 and NaPFO have similar values for both A_{cmc} and Γ_{cmc} . Different thicknesses are expected due to DynaxTM DX1030 having the additional CH_2

groups. DynaxTM DX1030 and CapstoneTM 1157 have a very similar overall molecular size and tail structure, therefore as expected comparable values are observed for fitted layer thickness (τ), $26.5 \pm 1.0 \text{ \AA}$ and $23.0 \pm 0.5 \text{ \AA}$ respectively. Although they are similar in size, differences are observed when considering both A_{cmc} and Γ_{cmc} , this being due to DynaxTM DX1030 being anionic and CapstoneTM 1157 zwitterionic. DynaxTM DX1030 has a larger area per molecule and thus lower surface excess to CapstoneTM 1157, due to charge repulsion between head groups [36]. Comparing ST and NR for CapstoneTM 1157, there are similarities between the values for both Γ_{cmc} and A_{cmc} : $\Gamma_{cmc} = 5.80 \pm 0.1 \times 10^{-6} \text{ mol m}^{-2}$ (ST) and $5.22 \pm 0.10 \times 10^{-6} \text{ mol m}^{-2}$ (NR), $A_{cmc} = 28 \pm 1 \pm 1 \text{ \AA}^2$ (ST) and $31 \pm 1 \text{ \AA}^2$ (NR). CapstoneTM 1157 was found to be the most amenable to tensiometric measurements and therefore analysis, see supporting information. Another important comparison to make is between the cross-sectional area of a single fluorocarbon chain, which is approximately 28 \AA^2 [37, 38, 39]. Well packed fluorocarbon surfactant monolayers generate a low limiting value of γ_{cmc} of 15 mN m^{-1} [5]. This value represents the physical limit at which these surfactant molecules can pack at an air-water interface, therefore leading to the lowest achievable value of γ_{cmc} . With this in mind, it is interesting to observe the easy to follow trend between A_{cmc} and limiting value of γ_{cmc} between the technical surfactants in this study. The molecule with the largest A_{cmc} (DynaxTM DX2200) has a γ_{cmc} of $\sim 20 \text{ mN m}^{-1}$ (Table S8, supporting information). CapstoneTM 1157 has the lowest A_{cmc} of the three technical surfactants (comparable to that of a single fluorocarbon chain), explaining the low observed γ_{cmc} of $\sim 16 \text{ mN m}^{-1}$ (Table S8, supporting information).

DynaxTM DX2200 is a non-ionic fluorosurfactant with a large head group of repeating acrylamide units. Due to its larger relative size compared to the two other surfactants, it is expected that DynaxTM DX2200 will have a smaller surface excess and a larger area per molecule, as reflected in the findings. As previously mentioned, properties of a non-ionic surfactant of similar structure to DynaxTM DX2200 have been reported in the literature [33]. Parameters derived from analysis of NR data provided comparable results for both Γ_{cmc} and A_{cmc} , $\Gamma_{cmc} = 2.50 \pm 0.10 \text{ mol} \times 10^{-6} \text{ m}^{-2}$ and $65.0 \pm 0.5 \text{ \AA}^2$ (Dynax DX2200), $\Gamma_{cmc} = 2.46 \times 10^{-6} \text{ mol m}^{-2}$ and 67 \AA^2 (THAM)-derived telomer).

Neutron reflectivity provides significant information on how these surfactants for fire-fighting applications, adsorb and pack at the air-water interface. Although this study has reported results on these FC surfactants as single surfactant systems, it provides a means for further investigations into more

Surfactant	$\rho/$ (10^{-6} \AA^2)	$\tau/$ (\AA)	$\Gamma_{cmc}/$ ($10^{-6} \text{ mol m}^{-2}$)	$A_{cmc}/$ (\AA^2)
NaPFO (This Study)	2.5	15.0 ± 0.5	4.05 ± 0.10	41 ± 2
NaPFO (Literature)	1.80	18.0 ± 0.5	4.00	42
Dynax TM DX1030	1.35	26.5 ± 1.0	3.95 ± 0.20	42.5 ± 2.0
Dynax TM DX2200	2.55	25 ± 2	2.50 ± 0.10	65.0 ± 0.5
Capstone TM 1157	2.00	23.0 ± 0.5	5.22 ± 0.10	31 ± 1

Table 2: Parameters from analysis of Neutron Reflection Data. ρ is the fitted scattering length density, τ the fitted monolayer thickness. Γ_{cmc} is the surface excess concentration at the CMC and A_{cmc} is the area per molecule at the CMC (Equation 4).

complex mixed systems, involving F Carbon/ F-Carbon and F-Carbon/ H-Carbon mixtures, as in real formulations. Overall, it has been shown that NR can be used to achieve consistent and reliable results for studying both research-grade and technical-grade FC surfactants. For the pure NaPFO, the data from both NR and tensiometric techniques were directly comparable to literature data. In addition to this, the three technical grade FC surfactants followed the expected trends in terms of τ , Γ_{cmc} and A_{cmc} , unlike the unexpected and erratic trends found using tensiometry.

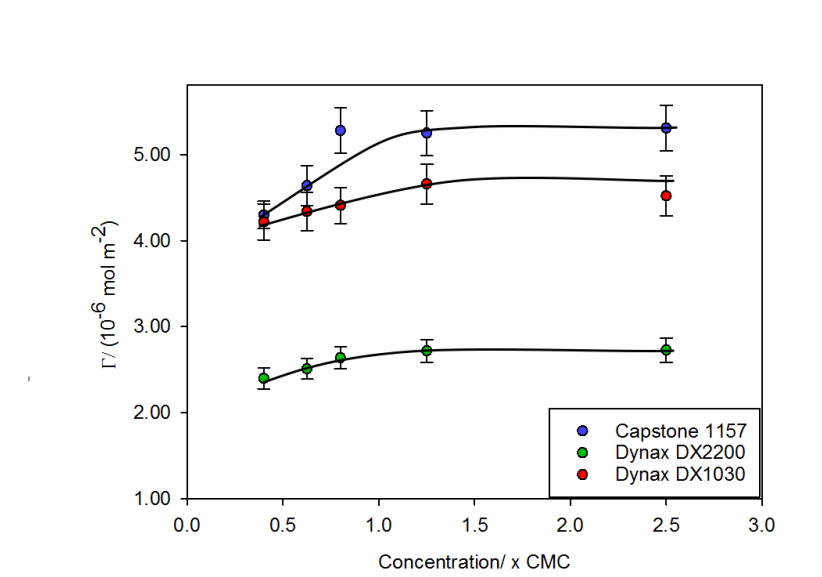
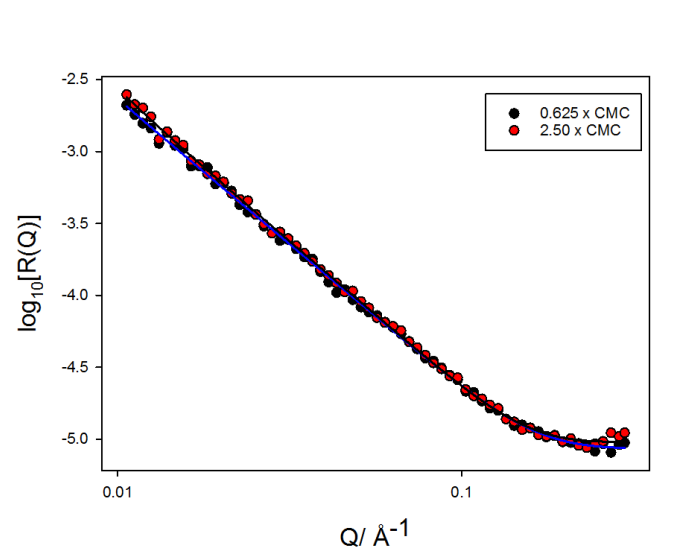


Figure 3: Above: CapstoneTM 1157 neutron reflection profiles to show difference in reflection intensity. Fitted functions shown as lines. Below: Surface excesses obtained by analysis of neutron reflection data. Lines are a guide to the eye. Critical micelle concentrations have been taken as 0.23 mM, 1.37 mM and 0.02 mM for CapstoneTM 1157, DynaxTM 1030 and DynaxTM DX2200 respectively. T= 25°C.

3.3. Small-Angle Neutron Scattering (SANS)

SANS has been employed to investigate self-assembly of the FC-surfactants. The surfactants were investigated over multiple concentrations above their respective CMCs (Table S3 in supporting information) at 25°C in D₂O. The micelle dimensions are given in Table 3 and 4 in the main text and the additional parameters including background and volume fraction are given in Tables S16 - S19 in the supporting information. The scattering profiles for all three surfactants are shown in Figure 4. The anionic surfactant, DynaxTM DX1030 (4a), and the non-ionic surfactant, DynaxTM DX2200 (4b), are well described by a form factor for oblate spheroids. Parameters for the oblate spheroid form factor are: equatorial radius ($R_{eq}/\text{Å}$), polar radius ($R_{pol}/\text{Å}$), aspect ratio ($X = R_{eq}/R_{pol}$) and charge (Z) for the anionic surfactant. The zwitterionic surfactant, Capstone 1157, displays scattering to much lower values of Q compared to the two other surfactants and these SANS curves have been fitted with a lamellar form factor. These aggregates have been modelling as infinite sheets of thickness ($T/\text{Å}$).

At low concentration (5 x CMC), DynaxTM DX1030 aggregates appear to be spherical in shape. Whereas, ellipsoidal aggregates are observed at 10 x CMC and above. The aspect ratio of the aggregates above 10 x CMC remain relatively stable ($X = 1.71 \pm 0.01$), suggesting that the shape of the micelles is not changing at these higher concentrations (Table 4). Another observation is that the structure factor $S(Q)$ peak for the anionic surfactant DynaxTM DX1030 which occurs at Q_{max} shifts to higher Q as the concentration is increased. At low concentrations, the $S(Q)$ peak is difficult to discern due to the weaker interactions. The Q_{max} peak provides a rough guide on the average distance between the micelles, through Equation 6. This shift to higher Q shows that there is a decrease in the average distance between the micelles with concentration. Similar results have been observed in studies of both anionic hydrocarbon and fluorocarbon surfactants [40, 41].

$$Q_{max} = 2\pi/d \quad (6)$$

The zwitterionic betaine, CapstoneTM 1157 has been studied at four different concentrations above its CMC. The solutions at these concentrations are quite viscous, reminiscent of viscoelastic systems, suggesting the formation of large and/or entangled aggregates. Amphoteric betaines are known to exhibit viscoelastic behaviour in solution, and work by Kumar *et al.* [42] showed by SANS/ TEM how a C22-amphoteric betaine generates worm-like

micelles thus resulting in the observed rheological properties.

In the low- Q region, the scattering scales as $I(Q) \approx Q^{-D}$, where D is a characteristic dimensionality of the dispersed colloids and the gradient of a log-log plot will be $-D$ [43]. In the case of non-interacting spheres, D should be zero in the low- Q region, for cylinders, $D=1$, and for disks/ lamellar structure $D = 2$. Capstone 1157 generates scattering with a clear Q^{-2} dependency, as shown in Figure 4c, and therefore can be attributed to lamellar structures across the concentration range studied here. Fitting the data to a lamellar model provides information only on the thickness of the layers. The average fitted thickness over all concentrations is $\sim 25 \text{ \AA}$, this value being roughly commensurate with the tip-to-toe length of two of the tail groups for this surfactant.

Considering the molecular structure of non-ionic DynaxTM DX2200, with a fluorinated tail group and repeating acrylamide unit head group, a complex core-shell model fit was investigated. The model would consist of a fluorinated tail micelle core ($\rho \sim 3 \times 10^{-6} \text{ \AA}^{-2}$) surrounded by a shell of acrylamide unit headgroups ($\rho \sim 1 \times 10^{-6} \text{ \AA}^{-2}$) contrasted against a D₂O continuum ($\rho \sim 6 \times 10^{-6} \text{ \AA}^{-2}$). Attempts to determine a model fit for the system using this approach provided unphysical values for parameters, suggesting that the internal structure of these micelles cannot be resolved by SANS. Several reasons may explain this: (1) Perhaps because there is only effectively a relatively small contrast step across the interface; (2) Blurring of the contrast step at the headgroup/D₂O interface due to hydration by D₂O; (3) H-D exchange of NH₂ groups. This loss of interfacial contrast has been noted before in SANS studies of both hydrocarbon and fluorocarbon hydroxy surfactants [33, 44], therefore this is likely here considering the acrylamide groups bear labile amide protons. Hence, here SANS has only been able to resolve an average contrast for the micellised surfactant against solvent and therefore an overall global fit has been conducted.

The self-assembled structure adopted by non-ionic DynaxTM DX2200 at all studied concentrations is best described by oblate spheroids, or globular micelles, with no observable structure factor over these concentrations and Q ranges. This is commonly seen for non-ionic fluorinated surfactants [33, 45]. From Table 4 it can be seen that on average the surfactant had an equatorial radius of 65 \AA and a polar radius of 28 \AA . The calculated tip-to-toe length of this molecule is $\sim 63 \text{ \AA}$, this therefore suggests that the molecule is fully extended at the extreme equatorial axis, but is coiled up at the extreme polar axis. This coiling has been previously observed using SANS in surfactants

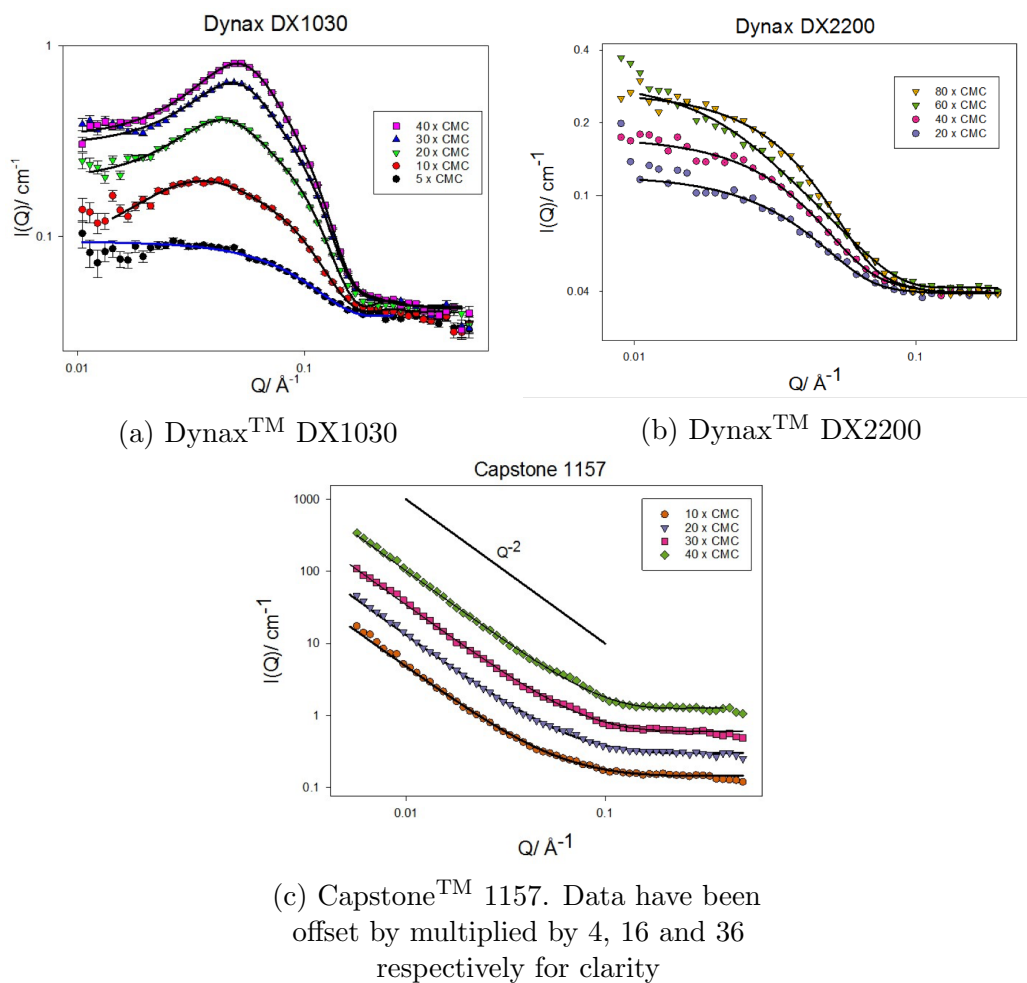


Figure 4: Small-angle neutron scattering profiles of the three surfactants and fitted functions shown as lines. Critical micelle concentrations have been taken as 0.23 mM, 1.37 mM and 0.02 mM for CapstoneTM 1157, DynaxTM 1030 and DynaxTM DX2200 respectively. T= 25°C.

containing polyoxyethylene groups [46], therefore is likely to occur with the oligomeric acrylamide moieties.

The different aggregate structures can be explained by consideration of the surfactant packing parameter argument (Equation 7):

$$P_C = v/(a_o l_c) \quad (7)$$

Where v is volume of the hydrophobic tails, a_o is head group area and l_c is the length of the hydrophobic chain. For each surfactant the tail volume and length effectively remains the same and the only factor changing is predominantly the head group area. As expected, the molecule with the largest headgroup (DynaxTM DX2200) formed ellipsoidal micelles, and the molecule with the smallest head group (CapstoneTM 1157) formed larger lamellar aggregates. Overall, three different self-assembled structures were observed for the three different fluorinated surfactants, highlighting how a change of surfactant headgroup can vastly affect self-assembly structure.

Surfactant	Concentration (x CMC)	SANS2D ISIS, UK					
		Model	R_{eq} (Å) (± 0.1)	R_{pol} (Å) (± 0.1)	Aspect ratio	N_{agg}	Z (± 1)
Dynax TM DX1030	5	Sphere	22.0	22.0		54	
	10	Ellipsoid	29.0	17.0	1.7	97	10
	20	Ellipsoid	28.5	16.7	1.7	92	7
	30	Ellipsoid	29.0	17.0	1.7	97	7
	40	Ellipsoid	30.0	17.7	1.7	108	8
Dynax TM DX2200	20	Ellipsoid	61.0	31.0	2.0	212	
	40	Ellipsoid	64.0	28.0	2.3	311	
	60	Ellipsoid	70.0	22.0	3.2	292	
	80	Ellipsoid	63.0	31.0	2.0	333	

Table 3: Parameters obtained by fitting SANS data to structural models. Information regarding models used for fittings can be found in the supporting information. R_{eq} is the equatorial radius of an ellipsoid, R_{pol} is the polar radius of the ellipsoid, aspect ratio is defined as $X = R_{eq}/R_{pol}$, N_{agg} is the aggregation number and Z is effective charge. Critical micelle concentrations have been taken as 1.37 mM and 0.02 mM for DynaxTM 1030 and DynaxTM DX2200 respectively. $T = 25^\circ\text{C}$.

Surfactant	Concentration (x CMC)	SANS2D ISIS, UK	
		Model	Thickness (Å) (±1)
Capstone™ 1157	10	Lamellar	22
	20	Lamellar	23
	30	Lamellar	26
	40	Lamellar	27

Table 4: Parameters obtained by fitting SANS data to a structural model for infinite lamellae. Information regarding models used for fitting can be found in the supporting information. **Critical micelle concentrations has been taken as 0.23 mM.** T= 25°C.

4. Conclusions

There are clear incentives to move away from the use of industrial fluorocarbon (FC) surfactants [3, 9, 10, 11, 12, 13, 47]. However, to practically achieve this, there must be an understanding of the important bulk and surface properties of these surfactants as both single and multi-component systems. Here, three typical industrial FC surfactants used in fire-fighting have been characterised by surface tension, fluorescence probe studies, neutron reflection and small-angle neutron scattering, so that links can be made between their structures and respective bulk and interfacial performance.

As expected, all surfactants have very low limiting surface tensions, with the lowest being observed for the zwitterionic surfactant ($\gamma_{CMC} = 15.6 \text{ mN m}^{-1}$). Comparisons in limiting surface tension and critical micelle concentrations (CMC) between partially fluorinated surfactants in this study and fully fluorinated surfactants (sodium perfluorooctanoate (NaPFO) [28]) have been made (Tables 1 and S8), with clear differences being noted. The CMC of NaPFO was found to be much higher (factor of 20 difference compared to the anionic partially fluorinated surfactant) and γ_{CMC} was higher also. In addition to this, it was interesting to note the differences in surface activity between the zwitterionic surfactant Capstone™ 1157 and the anionic surfactant Dynax™ DX1030. Although they both have the same tail structure, but only differ in head group, the zwitterionic surfactant has a CMC ~ 6 times lower and a $\gamma_{CMC} \sim 4 \text{ mN m}^{-1}$ lower than the anionic surfactant. These results show how considerable changes in the interfacial properties of surfactants result from changes in surfactant chemical structure.

In depth analysis of the surface tension data using the Gibbs adsorption

isotherm was prevented due to possible contamination owing to the commercial nature of these surfactants. In an attempt to circumvent this problem, neutron reflection was used to gain understanding of the surfaces, by determining parameters such as surface excess and area per molecule. The range of surfactants used in this provided an easy to follow expected trend, largest area per molecule (A_{cmc}) was observed in the largest molecule non-ionic DynaxTM DX2200, and smallest A_{cmc} in the smallest molecule zwitterionic CapstoneTM 1157. Again it is interesting to see the differences when comparing the zwitterionic to the anionic surfactant. The charge on the anionic surfactant feeds through to an increase of $\sim 12 \text{ \AA}^2$ in A_{cmc} and a $\sim 1.2 \times 10^{-6} \text{ mol m}^{-2}$ decrease in Γ_{cmc} . Another important observation was that the monolayer of CapstoneTM 1157 appears to be comparable to that of a single fluorocarbon chain ($\sim 28 \text{ \AA}^2$) [37, 38, 39], suggesting that the molecules are reaching the limit at which they can physically position at the air-water interface, further explaining why this molecule has such a low value of γ_{cmc} ($\sim 15.6 \text{ mN m}^{-2}$). There has been much literature produced on NaPFO [28, 29, 35] and although it was possible to make comparisons between NaPFO and anionic DynaxTM DX1030/ CapstoneTM 1157, it was instructive to compare results from these technical grade surfactants and standards from literature. Dupont *et al.* [33] carried out experiments on a novel FC telomer surfactant, similar to DynaxTM DX2200 used in this study, which was used for comparison. For practical applications, it is important to have an understanding not only on the interfacial properties, but also bulk properties. An understanding of the bulk properties are important because links between self-assembly and rheology (viscoelasticity) can be made.

Through the use of small-angle neutron scattering (SANS) it has been possible to explore self-assembly structures. The differences observed in aggregation and self-assembly could be understood in terms of the packing parameter (Equation 7). Large head group surfactants (DynaxTM DX2200 and DynaxTM DX1030) resulted in scattering consistent with spherical or ellipsoidal form factors, whereas the small head group surfactant (CapstoneTM 1157) was better described by a lamellar-type form factor. CapstoneTM 1157 has been noted to be the only surfactant to display a noticeable increase of viscosity in solution, as previously reported by Kumar *et al.* [42] with similar FC zwitterionic surfactants. By having this understanding of how these surfactants self-assemble individually, more complex studies can be proposed to model systems closer to practical applications, i.e containing F/F Carbon or H/F Carbon surfactant mixtures.

This study has highlighted some of the important surfactant properties for fire-fighting application, notably for aqueous film-forming foams (AFFFs). Surfactants with low surface tensions and CMCs are likely to perform better and provide a way of achieving the desired interfacial properties. As well as this, results have shown the sensitivity between the relationship of structure and performance between surfactants with similar tail groups but different head groups. This emphasises how changes in a head group can provide a large difference in both bulk and surface behaviour. In addition, it has been shown how lab-based tensiometric techniques are not always reliable for analysis of technical grade FC surfactants. However, the utility of neutron reflection for systems and studies of this kind has been demonstrated. These results therefore provide important insight into structure-performance relationships in FC surfactants, and will point towards new ways to design more environmentally benign and effective FC surfactants in the future.

Acknowledgements

CH thanks Angus Fire Ltd. for the provision of a PhD studentship. The authors thank the UK Science and Technology Facilities Council (STFC) for allocation of beamtime at ISIS and ILL and associated grants for consumables and travel. This work benefited from SasView Small Angle Scattering Analysis Software Package, originally developed by the DANSE project under NSF award DMR-0520547.

References

- [1] A. Ratzler, History and development of foam as a fire extinguishing medium, *Industrial and Engineering Chemistry* 48 (11) (1956) 2013–2016.
- [2] C. Hill, J. Eastoe, Foams: From nature to industry, *Advances in Colloid and Interface Science* 247 (2017) 496 – 513. doi:<https://doi.org/10.1016/j.cis.2017.05.013>.
- [3] C. A. Moody, J. A. Field, Perfluorinated surfactants and the environmental implications of their use in fire-fighting foams., *Environmental Science and Technology* 34 (18) (2000) 3864–3870.
- [4] A. Czajka, G. Hazell, J. Eastoe, Surfactants at the design limit, *Langmuir* 31 (30) (2015) 8205–8217.
- [5] M. P. Krafft, J. G. Riess, Chemistry, physical chemistry, and uses of molecular fluorocarbon- hydrocarbon diblocks, triblocks, and related compounds unique apolar components for self-assembled colloid and interface engineering, *Chemical Reviews* 109 (5) (2009) 1714–1792.
- [6] W. D. Harkins, A. Feldman, Films. the spreading of liquids and the spreading coefficient, *Journal of the American Chemical Society* 44 (12) (1922) 2665–2685.
- [7] K. Shinoda, T. Nomura, Miscibility of fluorocarbon and hydrocarbon surfactants in micelles and liquid mixtures. basic studies of oil repellent and fire extinguishing agents, *The Journal of Physical Chemistry* 84 (4) (1980) 365–369.

- [8] B. Z. Dlugogorski, S. Phiyalaninmat, E. M. Kennedy, Dynamic surface and interfacial tension of AFFF and fluorine-free Class B foam solutions, *Fire Safety Science* 8 (2005) 719–730.
- [9] M. Filipovic, A. Woldegiorgis, K. Norström, M. Bibi, M. Lindberg, A.-H. Österås, Historical usage of aqueous film forming foam: A case study of the widespread distribution of perfluoroalkyl acids from a military airport to groundwater, lakes, soils and fish, *Chemosphere* 129 (2015) 39–45.
- [10] W. J. Backe, T. C. Day, J. A. Field, Zwitterionic, cationic, and anionic fluorinated chemicals in aqueous film forming foam formulations and groundwater from US military bases by non-aqueous large-volume injection HPLC-MS/MS, *Environmental Science and Technology* 47 (10) (2013) 5226–5234.
- [11] B. J. Place, J. A. Field, Identification of novel fluorochemicals in aqueous film-forming foams used by the US military, *Environmental Science and Technology* 46 (13) (2012) 7120–7127.
- [12] J. Giesy, K. Kannan, Perfluorochemical surfactants in the environment, *Environmental Science and Technology* 36 (7) (2002) 146A.
- [13] J. Seow, C. W. Australia, Fire Fighting Foams with Perfluorochemicals-Environmental Review, 2013.
- [14] K. M. Hinnant, M. W. Conroy, R. Ananth, Influence of fuel on foam degradation for fluorinated and fluorine-free foams, *Colloids and Surfaces A: Physicochemical and Engineering Aspects* 522 (2017) 1–17.
- [15] L. A. DAgostino, S. A. Mabury, Identification of novel fluorinated surfactants in aqueous film forming foams and commercial surfactant concentrates, *Environmental Science and Technology* 48 (1) (2013) 121–129.
- [16] D. Korolchenko, S. Voevoda, Influence of spreading structure in an aqueous solution-hydrocarbon system on extinguishing of the flame of oil products, in: *MATEC Web of Conferences*, Vol. 86, EDP Sciences, 2016, p. 04038.

- [17] J. D. Hines, The preparation of surface chemically pure sodium n-dodecyl sulfate by foam fractionation, *Journal of Colloid and Interface Science* 180 (2) (1996) 488–492.
- [18] J. Eastoe, S. Nave, A. Downer, A. Paul, A. Rankin, K. Tribe, J. Penfold, Adsorption of ionic surfactants at the air - solution interface, *Langmuir* 16 (10) (2000) 4511–4518.
- [19] J. Lu, E. Lee, R. Thomas, J. Penfold, S. Flitsch, Direct determination by neutron reflection of the structure of triethylene glycol monododecyl ether layers at the air/water interface, *Langmuir* 9 (5) (1993) 1352–1360.
- [20] J. Hines, P. Garrett, G. Rennie, R. Thomas, J. Penfold, Structure of an adsorbed layer of n-dodecyl-N, N-dimethylamino acetate at the air/solution interface as determined by neutron reflection, *The Journal of Physical Chemistry B* 101 (36) (1997) 7121–7126.
- [21] H. Xu, P. Li, K. Ma, R. J. Welbourn, J. Penfold, D. W. Roberts, R. K. Thomas, J. T. Petkov, Adsorption of methyl ester sulfonate at the air-water interface: Can limitations in the application of the gibbs equation be overcome by computer purification?, *Langmuir* 33 (38) (2017) 9944–9953.
- [22] Ö. Topel, B. A. Çakır, L. Budama, N. Hoda, Determination of critical micelle concentration of polybutadiene-block-poly (ethyleneoxide) diblock copolymer by fluorescence spectroscopy and dynamic light scattering, *Journal of Molecular Liquids* 177 (2013) 40–43.
- [23] J. Webster, S. Holt, R. Dalglish, INTER the chemical interfaces reflectometer on Target Station 2 at ISIS, *Physica B: Physics of Condensed Matter* (385-386) (2006) 1164–1166.
- [24] A. Nelson, Co-refinement of multiple-contrast neutron/X-ray reflectivity data using MOTOFIT, *Journal of Applied Crystallography* 39 (2) (2006) 273–276.
- [25] J. Daillant, A. Gibaud, X-ray and neutron reflectivity: principles and applications, Vol. 770, Springer, 2008.

- [26] J. Penfold, R. Thomas, The application of the specular reflection of neutrons to the study of surfaces and interfaces, *Journal of Physics: Condensed Matter* 2 (6) (1990) 1369.
- [27] Z. Derikvand, M. Riazi, Experimental investigation of a novel foam formulation to improve foam quality, *Journal of Molecular Liquids* 224 (2016) 1311–1318.
- [28] E. Kissa, *Fluorinated surfactants and repellents*, Vol. 97, CRC Press, 2001.
- [29] J. Lu, R. Ottewill, A. Rennie, Adsorption of ammonium perfluorooctanoate at the air–water interface, *Colloids and Surfaces A: Physicochemical and Engineering Aspects* 183 (2001) 15–26.
- [30] S. K. Hait, S. P. Moulik, Determination of critical micelle concentration (CMC) of non-ionic surfactants by donor-acceptor interaction with iodine and correlation of CMC with hydrophile-lipophile balance and other parameters of the surfactants, *Journal of Surfactants and Detergents* 4 (3) (2001) 303–309.
- [31] P. H. Elworthy, K. J. Mysels, The surface tension of sodium dodecylsulfate solutions and the phase separation model of micelle formation, *Journal of Colloid and Interface Science* 21 (3) (1966) 331–347.
- [32] K. J. Mysels, Surface tension of solutions of pure sodium dodecyl sulfate, *Langmuir* 2 (4) (1986) 423–428.
- [33] A. Dupont, J. Eastoe, P. Barthélémy, B. Pucci, R. Heenan, J. Penfold, D. C. Steytler, I. Grillo, Neutron reflection and small-angle neutron scattering studies of a fluorocarbon telomer surfactant, *Journal of Colloid and Interface Science* 261 (1) (2003) 184–190.
- [34] S. An, J. Lu, R. Thomas, J. Penfold, Apparent anomalies in surface excesses determined from neutron reflection and the gibbs equation in anionic surfactants with particular reference to perfluorooctanoates at the air/water interface, *Langmuir* 12 (10) (1996) 2446–2453.
- [35] E. A. Simister, E. M. Lee, J. R. Lu, R. K. Thomas, R. H. Ottewill, A. R. Rennie, J. Penfold, Adsorption of ammonium perfluorooctanoate

- and ammonium decanoate at the air/solution interface, *Journal of the Chemical Society, Faraday Transactions* 88 (20) (1992) 3033–3041.
- [36] E. Lee, R. Thomas, J. Penfold, R. Ward, Structure of aqueous decyltrimethylammonium bromide solutions at the air water interface studied by the specular reflection of neutrons, *The Journal of Physical Chemistry* 93 (1) (1989) 381–388.
- [37] J. Eastoe, A. Paul, A. Rankin, R. Wat, J. Penfold, J. R. Webster, Fluorinated non-ionic surfactants bearing either CF₃ or H-CF₂ - terminal groups: Adsorption at the surface of aqueous solutions, *Langmuir* 17 (25) (2001) 7873–7878.
- [38] A. Downer, J. Eastoe, A. R. Pitt, J. Penfold, R. K. Heenan, Adsorption and micellisation of partially-and fully-fluorinated surfactants, *Colloids and Surfaces A: Physicochemical and Engineering Aspects* 156 (1-3) (1999) 33–48.
- [39] C. Arrington Jr, G. Patterson, Colloidal properties of highly fluorinated alkanolic acids, *The Journal of Physical Chemistry* 57 (2) (1953) 247–250.
- [40] E. G. R. Putra, A. Ikram, Nanosize structure of self-assembly sodium dodecyl sulfate: A study by small-angle neutron scattering (SANS), *Indonesian Journal of Chemistry* 6 (2) (2010) 117–120.
- [41] S. S. Berr, R. R. Jones, Small-angle neutron scattering from aqueous solutions of sodium perfluorooctanoate above the critical micelle concentration, *The Journal of Physical Chemistry* 93 (6) (1989) 2555–2558.
- [42] R. Kumar, G. C. Kalur, L. Ziserman, D. Danino, S. R. Raghavan, Wormlike micelles of a C22-tailed zwitterionic betaine surfactant: from viscoelastic solutions to elastic gels, *Langmuir* 23 (26) (2007) 12849–12856.
- [43] D. S. Sivia, *Elementary scattering theory: for X-ray and neutron users*, Oxford University Press, 2011.
- [44] J. Eastoe, P. Rogueda, A. M. Howe, A. R. Pitt, R. K. Heenan, Properties of new glucamide surfactants, *Langmuir* 12 (11) (1996) 2701–2705.

- [45] L. K. Shrestha, S. C. Sharma, T. Sato, O. Glatter, K. Aramaki, Small-angle x-ray scattering (SAXS) study on non-ionic fluorinated micelles in aqueous system, *Journal of Colloid and Interface Science* 316 (2) (2007) 815–824.
- [46] P. A. FitzGerald, T. W. Davey, G. G. Warr, Micellar structure in gemini non-ionic surfactants from small-angle neutron scattering, *Langmuir* 21 (16) (2005) 7121–7128.
- [47] A. V. Vinogradov, D. Kuprin, I. Abduragimov, G. Kuprin, E. Serebriyakov, V. V. Vinogradov, Silica foams for fire prevention and fire-fighting, *ACS Applied Materials and Interfaces* 8 (1) (2016) 294–301.